Analysis of Thermomechanical Cracks of Disc Brake Used in Heavy Trucks

Welteji Bena[1], Hirpa G. Lemu[2]

Abstract – *In the present work, the study of fatigue failure of the disc brake of Volvo truck under thermomechanical effects across the disc thickness is reported. Both analytical and numerical approaches have been used. In the analytical approach, flat rigid asymmetric punch contact behavior was assumed at surface interaction, while in the numerical approach, the 3D finite element model of the vented disc type is subjected to thermomechanical cycles using ABAQUS software. Linear elastic material models were used to simulate the material's behavior under the applied pad pressure on the disc. Surface-to-surface type of contact was used for bodies that have arbitrary shapes with relatively large contact areas at disc pad interfaces. The crack initiated due to hydraulic pressure of 1.47 MPa on the disc was analyzed under mixed-mode (mode I and II) conditions. This analysis has shown that the crack propagated up to critical length of 6.02 mm and finally, failure of the disc brake was observed.*

Keywords: *Fatigue, disc brake, thermal gradient, thermomechanical stress, thermal contact*

List of symbols

T_∞	Ambient Temperature
ω	Angular velocity of disc
σ	Applied remote stress
t_b	Braking time
ε_θ	Circumferential deformation strain
α	Coefficient of linear thermal expansion
a	Crack length
ρ	Density
Δk_{eq}	Equivalent stress intensity factor
ε'_f	Fatigue ductility
N_f	Fatigue life
FP	Fatigue parameter
Y(a)	Geometrical correction factor
P	Hydraulic pressure
σ_θ	Normal stress in circumferential direction
σ_r	Normal stress in radial direction
N_i	Number of cycles for crack initiation
C	Paris law crack-growth constant
m	Paris law crack-growth exponent
v	Poisson's ratio
P(r)	Pressure distribution
ε_r	Radial deformation strain
r, θ, z	Radial, circumferential and axial coordinates
$\gamma_{r\theta}$	Shear deformation strain
τ_f'	Shear fatigue strength coefficient
$\tau_{r\theta}$	Shearing stress in rθ plane
b	Strain life constant
K_I	Stress intensity factor of mode I crack
K_{II}	Stress intensity factor of mode II crack
ΔT	Temperature gradient
k	Thermal conductivity
t	Time
ε_t	Total strain
σ'_f	True stress
σ_y	Yield strength material
E	Young's modulus

I. Introduction

The brake system is used for safety control of a vehicle during braking and enables smooth stop of the vehicle within the shortest possible braking distance. The brake system is a crucial system particularly in stopping the heavy trucks in all moving stages including braking during high speed driving, sharp cornering, downhill driving, and repeated braking under normal operation and emergencies [1]. During sudden braking, a large force is applied and generates a large amount of heat energy at the interface of the disc-pad. In this condition, the kinetic energy of the vehicle is transformed into heat energy via friction between the rotor and the brake pad and dissipating the heat to the surrounding via the mode of heat transfer. Part of the heat is dissipated from the disc brake by conduction, while the remaining is dissipated to the surrounding atmosphere by convection and radiation [2]–[4].

Brake systems dissipate heat through a combination of different parts of its assembly such as brake pad, caliper, piston and rotor (Figure 1 [5]). In the braking process, the caliper clamps on disc rotor, which is the rotating part of the brake assembly, to slow the rotation, and then slow down or stop the vehicle. The two commonly employed

Manuscript received January 2007, revised January 2007

disc types are the solid type and the ventilated type. The former type is heavier in weight and used for less powerful vehicles, while the later type has holes on its surface and hence has rapid cooling effect. This makes the ventilated type applicable for a heavily loaded disc. The calipers house pistons and brake pads, which are key parts because they are the parts that contact and apply pressure and friction to a vehicle's brake rotor [6].

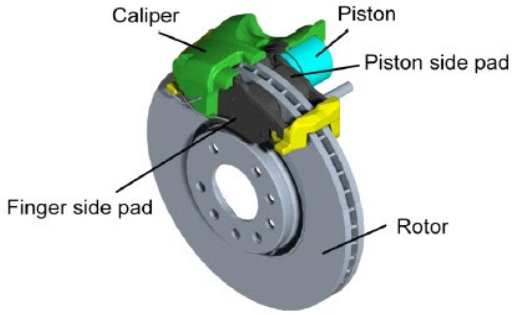

Fig. 1. Schematic diagram of the disc brake system

Brakes are sometimes operated at a thermal load that is above the allowable loading limit, which implies that proper selection of material for the brake disc and the temperature range of its functionality is important [7]. During the braking cycle, the thermal gradient is generated through the thickness of the disc due to heat dissipation. As the result, compressive stresses are induced on both sides of the disc. After releasing the brake, an outer surface is cooled and generates tensile stresses. Due to the thermal expansion and contraction, high thermomechanical stresses are induced along the radial, circumferential and axial directions [8].

Stress cycles with large amplitudes are formed as a result of repetitive stress-strain history. Such cycles could lead to low cycle fatigue cracks in the course of a few braking cycles. Changes in material microstructure lead to initiation and propagation of the cracks in the radial direction of the brake disc surface and hence significantly influencing the performance of the disc brake [9],[10]. Compared to passenger vehicles, thermal crack in trucks is very common due to its braking system, which goes through large braking load leading to radial thermal cracks (Figure 2 [10]).

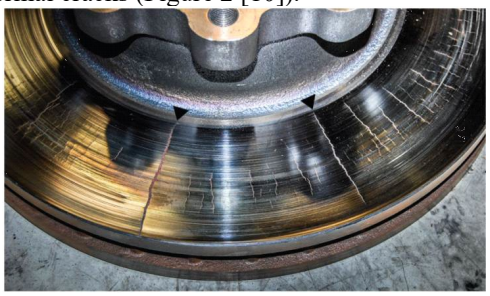

Fig. 2. Radial thermal cracks due to hard braking in heavy vehicle

Continuous crack propagation finally results in the total damage of disc brake which may cause serious accidents, deterioration of brake performance and an increase in maintenance costs due to the necessity for the frequent exchange of brake pad and disc [11]. For the crack formation of disc material, a few studies are reported on use of numerical methods. Zaid et al., [12] studied the temperature distribution on ventilated disc brake rotor of passenger vehicles with full load capacity by using ABAQUS/CAE and they observed transient response from the thermal analysis. Temperature gradient of the contact areas is larger than that of the non-contact areas, and the distribution of temperature in all directions is not symmetrical [13, 14].

Belhocine and Afzal [15] presented on numerical simulation of thermo-mechanical behaviour of automotive braking system during stop braking based on CFD analysis. The results indicated that the total deformation, stress and temperature in the disc and contact pressure in the pads increase appreciably as a result of thermal stresses that are acting in addition to the mechanical stresses during the braking process. These become causes of the fatigue crack propagation in braking systems. Yildiz and Duzgun [16] studied the stress of ventilated brake discs by using finite element analysis (FEA) approach and found that stresses reduced on ventilated disc type having holes on its surface. Hence, the approach could be an improvement for eliminating crack formations [17].

Moghanlou and Assist [18] used ABAQUS software to investigate a three-dimensional model of a braking cycle, including braking and cooling, which causes high circumferential cyclic thermal stresses in brake discs of heavy-duty vehicles. Multiaxial characters of thermomechanical fatigue damage on the high-speed railway brake disc was studied by Lu et al. [19]. The stress and strain items for fatigue evaluation led to an underestimation of the brake disc thermomechanical fatigue damage read from results of simulation. Han et al. [20] have also analyzed thermal fatigue stress of automotive brake discs by using coupled thermomechanical finite element (FE) simulation. The braking fatigue cycles of the friction surface and the bolt holes were derived from Basquin and Coffin-Manson equations. The fatigue life of gray cast iron brake disc material had either an LCF or HCF depending on the temperature increase, based on the strain-life relationship. The variations during braking and cooling cycles would be the major cause in the initiation and propagation of surface radial cracks. Generally, the crack propagation rate of disc brake depends on disc geometry (solid or ventilated), temperature distribution and loading conditions [10].

This study focuses on disc brake fatigue failure analysis of Volvo truck under thermomechanical effect. The numerical approach is employed to simulate material behavior under temperature distribution through disc thickness. The aim is to identify the position of stress concentration where contact fatigue can be initiated. The contact behavior was flat rigid asymmetric punch with frictionless assumed flat disc interaction. Smith Watson model is used to estimate crack initiation while crack propagation is calculated by Paris law. The study is also aimed to determine the magnitude of the stresses and deformations, as well as the size of the contact area. Finally, the analytical results are compared with the

numerical results obtained using the commercial software ABAQUS, and the results are discussed.

The remaining part of the article is divided into 5 sections. After presenting the materials and methods used in the study in Section II, Section III and Section IV present the analytical analysis and the numerical (FEA) results respectively. Then, the analytical and numerical results are compared and discussed in Section V followed by the conclusions summarized in Section VI.

II. Materials and Methods

In the thermomechanical crack analysis, the properties of the linear elastic material of the disc brake are considered. Gray cast iron material is commonly for disc rotor and pads because it provides good wear resistance, gives excellent thermal conductivity, has good property to absorb and dissipate heat, serves in cooling the brakes and has the capacity to damp vibrations [21], [22].

Cast iron consists of graphite (carbon) flakes and matrix ferrous metal, which influence the stress-strain response of the material. This is because of the weak bonding between the graphite flakes and metal matrix that causes gaps or voids to open in the material under tension. In addition, the content of graphite provides important properties such as dimension stability under different heating conditions and high vibration damping. In this work, 3D modeling of the automotive disc brake was done in SOLIDWORKS and its cross-section view is shown in Figure 3. The overview of gray cast iron classifications and its mechanical properties are shown in Table 1 [23], [24].

TABLE I. *THERMO-PHYSICAL PROPERTIES OF GRAY CAST IRON*

Material properties	**Symbol**	**Pad**	**Disc**
Thermal conductivity, (W/m °C)	k	5	57
Density, (kg/m^3)	ρ	1400	7250
Poisson's ratio	v	0.25	0.28
Thermal expansion, (10^{-6} / °C)	α	10	10.38
Operation condition			
Angular velocity (rad/s)	ω		123
Hydraulic pressure (MPa)	P		1.47

Thermomechanical analysis of the disc brake required the condition of braking as input data. Volvo heavy truck was selected and the following conditions were assumed for the disc brake's braking condition.

(i). The average stopping distance of a truck is 73.45 m with the deceleration rate of 4.89 m/s^2 in braking time 5.48 s.

(ii). The ambient temperature of T_∞ = 27 °C.

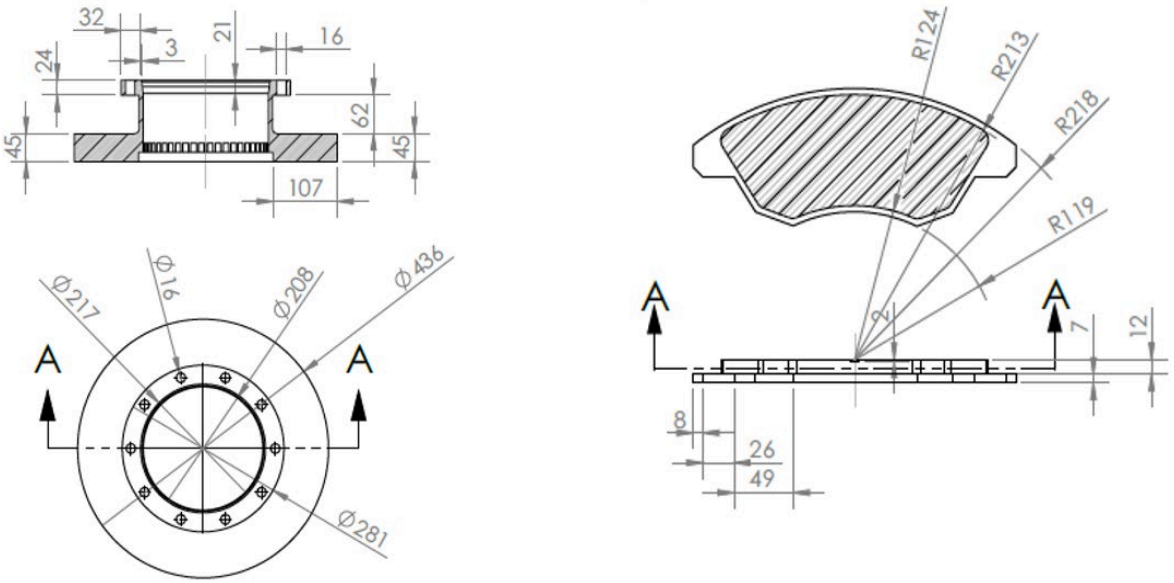

Fig. 3. Cross-section views of a ventilated disc brake and its pads

In addition, the following assumptions were used in disc brake analysis.

- The disc material is considered homogeneous and isotropic.
- At the disc brake rotor surface, all kinetic energy is converted to frictional heat or heat flux.
- The contact pressure is uniformly distributed over all friction surfaces hence the heat generation of the midplane is considered symmetric.

III. Analytical Analysis

III.1. Structural Analysis of Contact Pressure

In the analytical analysis of contact pressure distribution of flat disc pad interaction, the contact behavior was assumed to be a frictionless flat rigid axisymmetric punch (rounded edge) as shown in Figure 4. But the problem consists of an elastic punch (pad) pressed onto the rotating-disc brake, idealized as an elastic half-plane (disc brake), which may, in general, be elastically dissimilar [25].

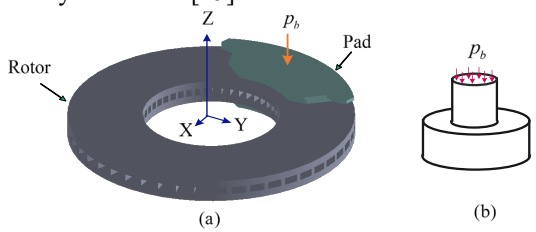

Fig. 4. Schematic of contact profile of flat rigid axisymmetric punch on flat disc

The radius of the pad, denoted by a, is assumed to be half of the difference between the outer and inner radius of the disc brake. The relation of normal pressure distribution P(r) and couple effect hydraulic pressure p_b applied on the disc is reduced to [26]:

$$p(r) = \frac{p_b}{\sqrt{1-\left(\frac{r}{a}\right)^2}} \quad (1)$$

Figure 5 illustrates the effects of the hydraulic pressure, P_b = 1.47 MPa (Table 1), at the contact edges where the stress distribution shows singular behavior, i.e. at the point where the value of stress is infinite. The maximum contact pressure and high stress occurred at the end of the surface of the punch.

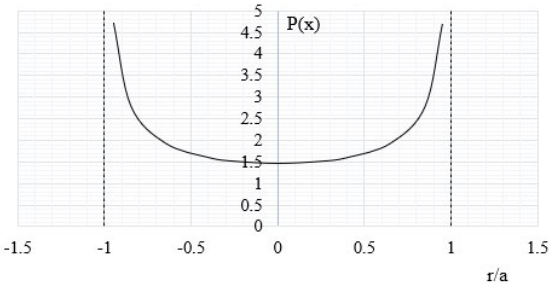

Fig. 5. Contact pressure distribution at the different surface of the punch

III.2. Thermomechanical stress distribution

The pressure in the brake pedals together with the system supports develop tensile force in the brake caliper, pressing the brake pads against the brake discs. Together with friction force at the contact interface, mechanical and thermal stresses on the disc and pads become high. To analyze the thermomechanical (TM) stress, it was assumed that the strain in axial direction was ignored because the frictional contact surface is at z = 0. The stress components acting on this plane are the radial stresses σrr, tangential (circumferential) stresses $\sigma_{\theta\theta}$ and the shear stresses $\tau_{r\theta}$. Thus, the disc deformation may be considered a 2D TM problem (Figure 6).

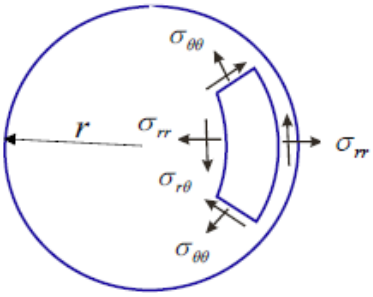

Fig. 6. Stress components in the 2D polar coordinate system

The stress-strain relationship for homogenous isotropic material by employing the generalized Hooks law of strain-based become [27], [28].

$$\sigma_r^{TM} = \frac{E}{(1+\nu)(1-2\nu)}[(1-\nu)\varepsilon_r + \nu\varepsilon_\theta - (1+\nu)\alpha\Delta T] \quad (2)$$

$$\sigma_\theta^{TM} = \frac{E}{(1+\nu)(1-2\nu)}[(1-\nu)\varepsilon_\theta + \nu\varepsilon_r - (1+\nu)\alpha\Delta T] \quad (3)$$

$$\tau_{r\theta}^{Me} = \frac{E}{2(1+\nu)}\gamma_{r\theta}^{Me} \quad (4)$$

Where ν is poison ratio, E is elastic modulus, ΔT temperature gradient, α is thermal diffusivity of the material, ε_{rr}, $\varepsilon_{\theta\theta}$ and $\gamma_{r\theta}$ are normal strain along radial, circumferential direction and shear strain on the r-θ plane respectively,

III.3. Thermo-mechanical fatigue of disc brake

Thermo-mechanical fatigue (TMF) is the combination of cyclical mechanical loading and cyclical thermal loading to cause material fatigue. Huge compressive stresses are generated in the circumferential direction of the disc brake surface, and this leads to plastic yielding. However, these compressive stresses are changed to tensile stresses as the disc cools down. Repetitive action of this type of stress-strain history with large amplitudes form could lead to low cycle fatigue cracks after a few braking cycles.

3.3.1. Fatigue cracks initiation modeling

Disc brakes that are widely used for heavy vehicle application are manufactured from gray cast iron of qualities GCI 25, which has high carbon content [21].
A higher carbon content improves the thermal conduction, which improves the ability to manage high brake power levels. The mechanical properties used in fatigue life calculation are given in Table 2 [29]. Smith Watson Topper damage Model [20] was better to estimate crack initiation of gray cast iron of disc brake material since it considers strain amplitude and maximum tensile stress. So, this model achieved for thermomechanical crack analysis compared to Basquin-

Manson-Coffin and Morrow Damage Model [30]. Equation 5 explains fatigue parameter (FP) of Smith Watson Topper damage Model.

$$FP = \frac{(\sigma_f')^2}{E}(2N_f)^{2b} + \sigma_f'\varepsilon_f'(2N_f)^{b+c} \quad (5)$$

Where $\sigma\left(\frac{\Delta\varepsilon}{2}\right)_{max}$, σ'_f is the true stress, N_f is fatigue life, E is modulus of elasticity, $\frac{\Delta\varepsilon_e}{2}$ elastic strain amplitude, ε'_f is the fatigue ductility, σ_{max} and σ_m maximum and mean stress respectively, b and c are slopes of elastic strains.

Substituting material properties into Eq. (5) of Smith Watson Topper model, damage parameters vs cycles of crack initiation can be plotted which is illustrated in Figure 7. The value of this model is used to determine the number of cycles to crack initiation. Therefore, the maximum fatigue parameter of 0.35 and the number of cycles 6.15×10^4 is obtained for the crack initiation.

TABLE II.
MECHANICAL PROPERTIES OF DISC BRAKE MATERIAL (GG25 GRAY CAST IRON)

E (GPa)	σ_y (MPa)	σ'_f (MPa)	ε'_f	b	c
138	206	241	0.864	-0.115	-0.771

3.3.2. The effect of the crack length on the stress intensity factors

The fatigue stress intensity factor K is used in fracture mechanics to forecast the state of the stress state near crack tip due to remotely loads or residual stresses. The magnitude of K depends on, among others, the sample geometry, the crack location and size as well as the magnitude and the modal distribution of the load. The stress intensity factor values at a special case of elliptical crack tip subjected to remote loading conditions under different modes are given by [31]:

$$k_I = \frac{2}{\pi}\sigma\sqrt{\pi a} \quad (6)$$

$$k_{II} = \frac{4}{\pi(2-\nu)}\sigma\sqrt{\pi a} \quad (7)$$

Where K_I and K_{II} are stress intensity factors for modes I and mode II or opening mode and shearing mode respectively, σ is the remotely applied stress, ν is the Poisson's ratio, and a is the half crack size.

This study focuses on the mixed-mode (I/II) loading, whose effective stress intensity factor (Δk_{eff}) is expressed as:

$$\Delta k_{eff} = (\Delta k_I^4 + 8\Delta k_{II}^4)^{\frac{1}{4}} \quad (8)$$

Figure 8 shows the influence of different crack lengths on the investigated intensity factor. On the pad selected for this analysis, a contact pressure of 1.47 MPa was applied over a crack length of 0.02 mm to 6.02 mm with the increments of 0.6 mm. The result showed that stress intensity factors (KI, KII and ΔKeq) increase as the crack length increases (Figure 8).

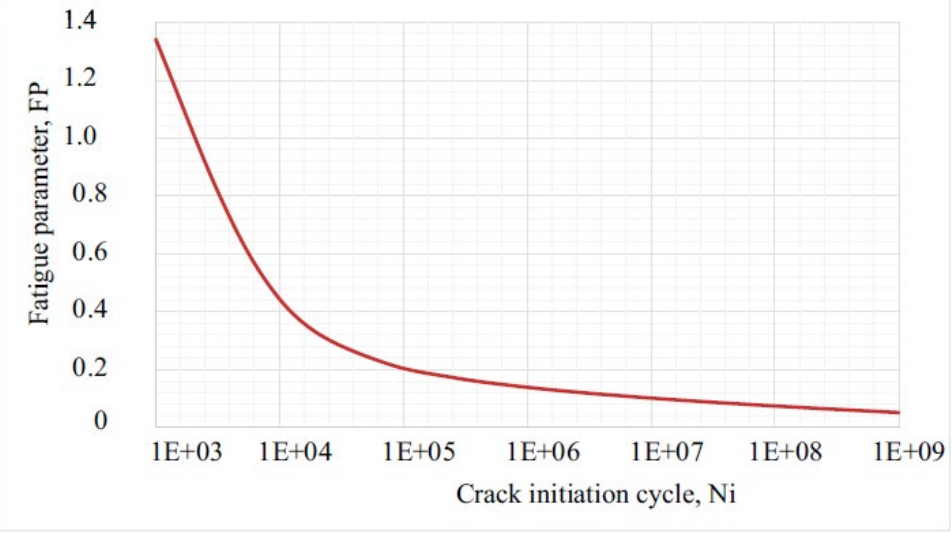

Fig. 7. Number of cycles to crack initiation (Ni) Vs different fatigue model

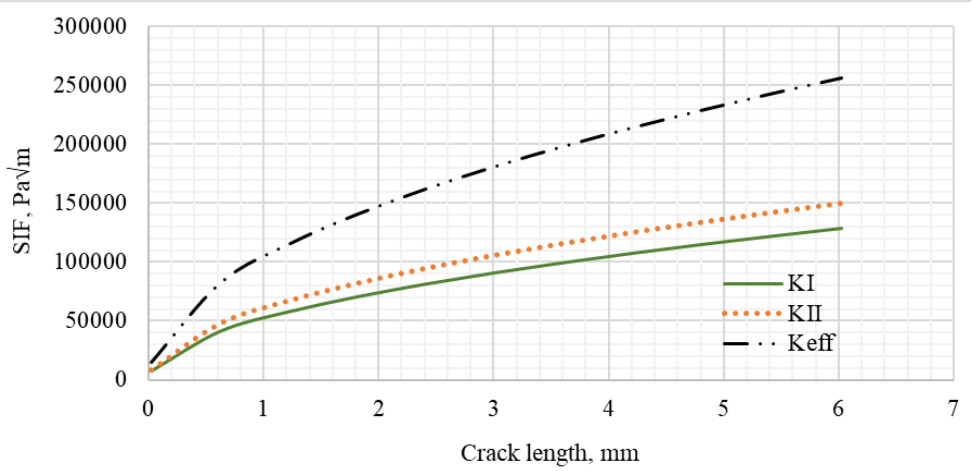

Fig. 8. Effects of crack length on stress intensity factor

3.3.3. Fatigue crack propagation

The cyclic tension and compression stress, which is in phase with brake temperature, is the thermomechanical load that leads to failure. This causes crack initiation followed by crack propagation. Crack propagation of the disc brake starts from the initiated crack growth up to the critical length of the crack. After the critical length, the crack propagates rapidly and finally, failure of the disc occurs. Analytically, the crack propagation is calculated by Paris law [22, 23].

$$N_f = \frac{2}{(m-2)CY^m \Delta\sigma^m}\left[\frac{1}{a_0^{\frac{(m-2)}{2}}} - \frac{1}{a_f^{\frac{(m-2)}{2}}}\right] \quad (9)$$

$$For,\ m \neq 2,\ a \gg a_0$$

Where $Y(a)$ geometrical correction factor, $\Delta\sigma$ is stress range, a_o and a_f are initial and final crack sizes respectively. The value of C and m are 5.5131e-12 and 3.3231 respectively, which are material constants of the disc brake [24]

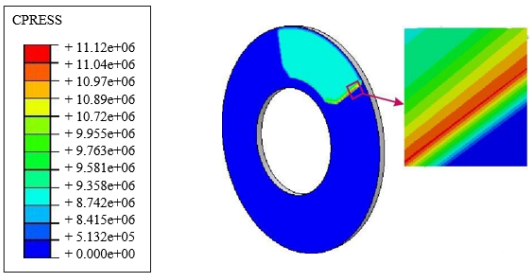

Fig. 9. Contour plot of contact pressure distribution on the disc

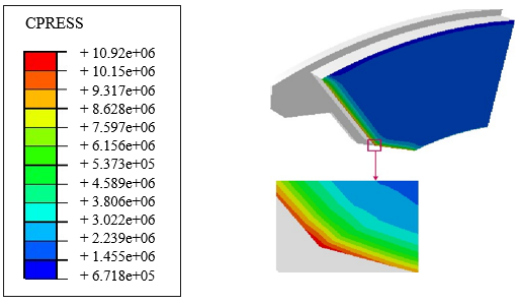

Fig. 10. Contour plot of contact pressure distribution on the pad

IV. FINITE ELEMENT ANALYSIS

IV.1. Contact pressure distribution

For the contact pressure distribution that took place at the rotor and pad interface, the transient temperature states accounted for. To ensure efficiency of the fine meshes, sub-modeling technique was employed. Figures 9 and 10 show the contact pressure distribution of the FEA sub-model for disc brake and pad, respectively when 1.47 MPa brake pressure was acting. The maximum contact pressure read from contour is 11.12 MPa and 10.92 MPa for the disc rotor and pad, respectively. This indicates that the maximum contact pressure appears on the edges of the entry part of the pad and continues down towards the exit from the area due to friction.

IV.2. von-Mises stress distribution

The induced high thermal gradient and stress state at the surface contacts of the disc are reduced through disc thickness. So, the surface and disc thickness are selected to analyze the stress distribution. The von Mises stress distribution in the disc-pad normal contact surface under the hydraulic pressure of 1.47 MPa is illustrated in Figure 11. From this figure, it is clearly observed that the maximum and the minimum von Mises stress distribution has occurred at the sharp edges. This is the main cause for the sub-surface fatigue crack initiation, which later propagates to the surface and causes disc brake failure.

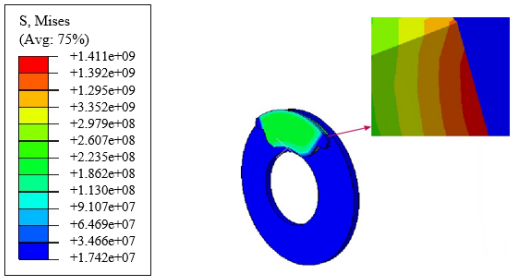

Fig. 11. Contour plot of von Misses stress distribution without temperature effect

V. DISCUSSIONS

V.1. Contact pressure distribution

In this section, analytical computation results are compared with finite element results. In the contact pressure analysis, the transient temperature distribution was considered in analytical and FEA methods. Figure 12 shows the results of the contact pressure distribution under application of 1.47 MPa pressure on the disc at the initial time of t = 0 s. At the initial pressing time until t = 1.5 s, the contact pressure was highly increasing then slightly dropped until the final braking time. As shown in the contour plots, the maximum value of the contact pressure by analytical and FEA methods are 11.34 MPa and 10.78 MPa respectively. Comparing the maximum contact pressure in both methods, percentage deviation of 2.50% is observed. This may be because of the course mesh size in the FEA. Both results of FEM and analytical method show geometrically similar shape.

V.2. von Mises stress distribution

von-Mises analysis across disc thickness under the applied brake pressure of 1.47 MPa is shown in Figure 13. Analytically, von Mises stress value was obtained using the values of radial, axial and circumferential stresses taken from equations (2) and (3). To solve the stress components, the values of radial and hoop strain became ε_θ = 0.002 and ε_r = 0.008 mm, which were estimated taking disc brake dimension from Table 1. The maximum stress of 1411 MPa by FEM and 1912 MPa by analytical method was read from the analysis results. Also, the figure depicts that the maximum von Misses stress is high at end edge of inner radius of disc in contact with pad brake because the stress concentration is high at the sharp edges. From this curve, it is clearly seen that the maximum von-Mises stress distribution occurs at the depth between 2 mm and 4 mm from the contact surface. This is the main cause for the sub-surface fatigue crack initiation, which later propagate to the surface and cause disc brake failure.

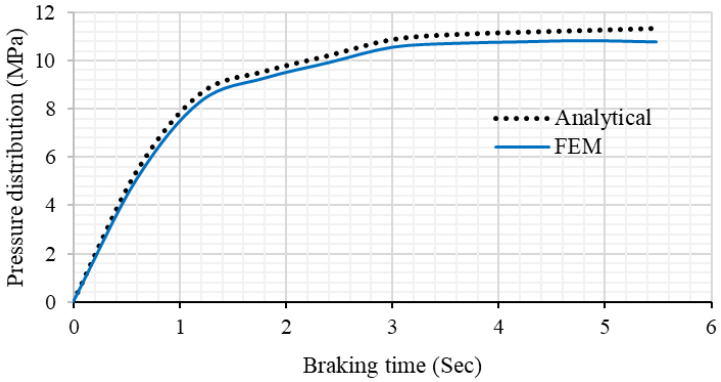

Fig. 12. Contact pressure distribution in the disc brake through braking time

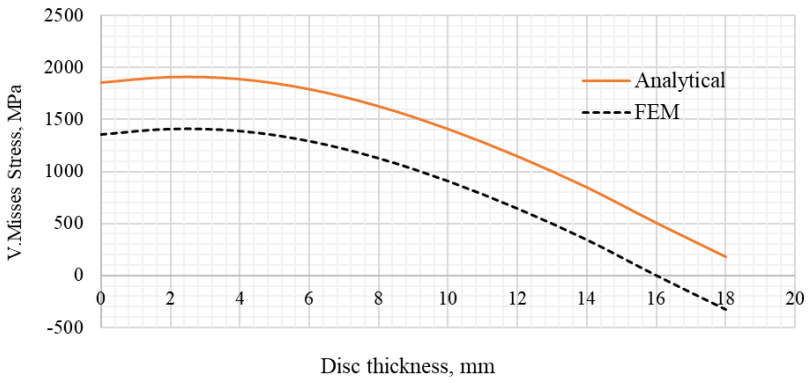

Fig. 13. Contour plot of von Mises stress distribution within disc brake system

V.3. Fatigue cracks propagation life

Crack propagation of the disc brake started from the initiated crack growth up to the critical length of the crack. Analytically, propagation was calculated by Paris law (Eq. 9). The crack length vs the number of cycles is illustrated in Figure 14. It showed that as the crack length increases, the number of cycles to failure also increases until it reaches the critical point. The critical crack length obtained from the analytical and FEA results are 6 mm and 5.54 mm respectively. The propagation life of the disc was 4324 cycles and 4305 cycles to failure by analytical and FEM approaches respectively. This number of cycles is the life of the disc from the initiated crack growth up to the critical length of the crack. After the critical length, the crack will propagate rapidly.

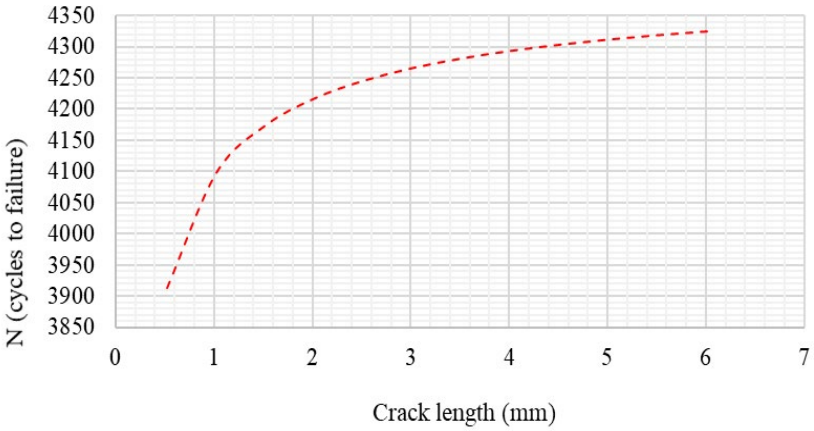

Fig. 14. Plot of fatigue life of the disc brake material

VI. CONCLUSIONS

The main intent of the study reported in this article is to perform thermo-mechanical crack analysis on ventilated disc type for heavy trucks. Both numerical and analytical approaches were employed to simulate material behavior under thermal gradient through the disc thickness. Defects formed at the points of high concentration due to cyclic heating and cooling at the contact zone of disc and pad cause the crack initiation. Crack initiation of gray cast iron of disc material was determined by the Smith Watson Topper model. The maximum fatigue parameter of 0.35 and the number of cycles of 6.15×10^4 were obtained for the crack initiation. Analytically, the number of cycles estimated for crack propagation was 4324 by modified Paris law. ABAQUS was used to analyze both thermomechanical stresses.

To reduce computation time, the sub-modeling system was used instead of full modeling. Additionally, to get more computational efficiency, the fine mesh was applied to the parts of the disc pad contact zone, and the coarse mesh was applied to other regions of the components. In this study, the maximum von Mises obtained from the FEA is 1411 MPa, found at a depth between 2 and 4 mm. The results showed that high thermal gradient through disc thickness and stress concentration at the rubbing surface causes crack initiation. This demonstrated the subsurface where the crack initiates and causes the fracture of the disc brake after a certain time.

Future research in this direction aims to improve the achieved results by developing a physical test model or an experimental test set-up on an existing truck that can help to validate the numerical model.

8 REFERENCES

[1] A. Belhocine and A. Afzal, “A predictive tool to evaluate braking system performance using a fully coupled thermo-mechanical finite element model,” *Int. J. Interact. Des. Manuf. IJIDeM*, vol. 14, no. 1, pp. 225–253, 2020.

[2] J. Qu, W. Wang, Z. Dong, and W. Shan, “Simulation Analysis and Verification of Temperature and Stress of Wheel-Mounted Brake Disc of a High-Speed Train,” *Chin. J. Mech. Eng.*, vol. 35, no. 1, pp. 1–9, 2022.

[3] T. Schneider, M. Dietsch, K. Voelkel, H. Pflaum, and K. Stahl, “Analysis of the Thermo-Mechanical Behavior of a Multi-Plate Clutch during Transient Operating Conditions Using the FE Method,” *Lubricants*, vol. 10, no. 5, p. 76, 2022.

[4] A. Belhocine and O. I. Abdullah, “Finite element analysis (FEA) of frictional contact phenomenon on vehicle braking system,” *Mech. Based Des. Struct. Mach.*, vol. 50, no. 9, pp. 2961–2996, 2022.

[5] A. Afzal and M. Abdul Mujeebu, “Thermo-mechanical and structural performances of automobile disc brakes: A review of numerical and experimental studies,” *Arch. Comput. Methods Eng.*, vol. 26, no. 5, pp. 1489–1513, 2019.

[6] A. Belhocine and O. I. Abdullah, “Design and thermomechanical finite element analysis of frictional contact mechanism on automotive disc brake assembly,” *J. Fail. Anal. Prev.*, vol. 20, no. 1, pp. 270–301, 2020.

[7] A. Modanloo and M. Talaee, “Analytical thermal analysis of advanced disk brake in high speed vehicles,” *Mech. Adv. Mater. Struct.*, vol. 27, no. 3, pp. 209–217, 2020.

[8] W. Sawczuk, M. Jüngst, D. Ulbrich, and J. Kowalczyk, “Modeling the Depth of Surface Cracks in Brake Disc,” *Materials*, vol. 14, no. 14, p. 3890, 2021.

Manuscript received January 2007, revised January 2007

[9] O. Grevtsev *et al.*, "Determination of Thermomechanical Stresses in Elements of Vehicles' Braking Systems," *Commun.-Sci. Lett. Univ. Zilina*, vol. 24, no. 1, pp. B1–B8, 2022.
[10] T. J. Mackin *et al.*, "Thermal cracking in disc brakes," *Eng. Fail. Anal.*, vol. 9, no. 1, pp. 63–76, 2002.
[11] B.Goo and C.Lim, "Thermal Fatigue of Cast Iron Brake Disc Materials," *J. Mech. Sci. Technol.*, vol. 26, no. 6, pp. 1719–24, 2012, 2012.
[12] M. Zaid, M. Radzai, R. Ahmad, M. Ridzuan, A. Nurfaizey, and M. Afzanizam, "An investigation of disc brake rotor by Finite element analysis," *J. Adv. Manuf. Technol.*, vol. 3, no. 2, pp. 37–48, 2009.
[13] Q. Jian and Y. Shui, "Numerical and experimental analysis of transient temperature field of ventilated disc brake under the condition of hard braking," *Int. J. Therm. Sci.*, vol. 122, pp. 115–123, 2017.
[14] Z. Wang, J. Han, X. Liu, Z. Li, Z. Yang, and E. Chen, "Temperature evolution of the train brake disc during high-speed braking," *Adv. Mech. Eng.*, vol. 11, no. 1, p. 1687814018819563, 2019.
[15] A. Belhocine and A. Afzal, "Computational finite element analysis of brake disc rotors employing different materials," *Aust. J. Mech. Eng.*, vol. 20, no. 3, pp. 637–650, 2022.
[16] Y. Yildiz and M. Duzgun, "Stress analysis of ventilated brake discs using the finite element method," *Int. J. Automot. Technol.*, vol. 11, no. 1, pp. 133–138, 2010.
[17] Y. Hong, T. Jung, and C. Cho, "Effect of Heat Treatment on Crack Propagation and Performance of Disk Brake with Cross Drilled Holes," *Int. J. Automot. Technol.*, vol. 20, no. 1, pp. 177–185, 2019.
[18] R. Moghanlou and M. Assist, "Three-dimensional Simulation of Thermal Stresses in Discs during an Automotive Braking Cycle," *Int. Sci. J.*, vol. 4, no. 3, pp. 158–61, 2018.
[19] C. Lu, J. Mo, R. Sun, Y. Wu, and Z. Fan, "Investigation into Multiaxial Character of Thermomechanical Fatigue Damage on High-Speed Railway Brake Disc," *Vehicles*, vol. 3, no. 2, pp. 287–299, 2021.
[20] M.-J. Han, C.-H. Lee, T.-W. Park, and S.-P. Lee, "Low and high cycle fatigue of automotive brake discs using coupled thermo-mechanical finite element analysis under thermal loading," *J. Mech. Sci. Technol.*, vol. 32, no. 12, pp. 5777–5784, 2018.
[21] O. Maluf, M. Angeloni, M. T. Milan, D. Spinelli, and W. W. Bose Filho, "Development of materials for automotive disc brakes," *Minerva*, vol. 4, no. 2, pp. 149–158, 2007.
[22] A. Belhocine and O. I. Abdullah, "Modeling and simulation of frictional disc/pad interface considering the effects of thermo-mechanical coupling," *World J. Eng.*, 2020.
[23] A. Belhocine and O. I. Abdullah, "Thermomechanical model for the analysis of disc brake using the finite element method in frictional contact," *Multiscale Sci. Eng.*, vol. 2, no. 1, pp. 27–41, 2020.
[24] A. Belhocine and A. Afzal, "Finite element modeling of thermomechanical problems under the vehicle braking process," *Multiscale Multidiscip. Model. Exp. Des.*, vol. 3, no. 1, pp. 53–76, 2020.
[25] J. K.L. and J. K.L., "Contact Mechanics," *Camb. Univ. Press*, 2003.
[26] S. Timeshenko and J. Goodier, "Theory of Elasticity," *McGraw-Hili*, vol. Second Edition, 1951.
[27] M. A. Tolcha and H. G. Lemu, "Modeling thermomechanical stress with H13 tool steel material response for rolling die under hot milling," *Metals*, vol. 9, no. 5, p. 495, 2019.
[28] I. T. Jiregna and H. G. Lemu, "Thermal stress analysis of disc brake using analytical and numerical methods," 2021, vol. 1201, no. 1, p. 012033.
[29] G. Le Gigan, *On improvement of cast iron brake discs for heavy vehicles*. Chalmers University of Technology, 2015.
[30] M. Rouhi Moghanlou and H. Saeidi Googarchin, "Three-dimensional coupled thermo-mechanical analysis for fatigue failure of a heavy vehicle brake disk: Simulation of braking and cooling phases," *Proc. Inst. Mech. Eng. Part J. Automob. Eng.*, vol. 234, no. 13, pp. 3145–3163, 2020.
[31] V. N. Rao, *Development of Simulation Methodology to Predict Crack Growth Behavior in Heavy Duty Truck Components using Full Vehicle Response Dynamic Loads*. North Carolina State University, 2016.

AUTHORS' INFORMATION

[1]Department of Mechanical Engineering, Mettu University, Ethiopia.
[2]Faculty of Science and Technology, University of Stavanger, N-4036 Stavanger, Norway.

Welteji Bena received his BSc degree in Mechanical Engineering from Jimma University in 2015 and M.Sc. degree in Mechanical Design from Jimma University, Ethiopia in 2020. Currently, he is a lecturer at Department of Mechanical Engineering, Mettu university. His research interests are studying sustainable energy source, effect of thermomechanical load in mechanical structures, Fracture mechanics, etc.

[2]Hirpa G. Lemu earned his MSc and PhD degrees from Norwegian University of Science and Technology (NTNU), Norway, in 1996 and 2002 respectively. Currently he is a Professor of Mechanical Design Engineering at University of Stavanger, Norway. His research activities and interests include design optimization, simulation-driven optimization, material behavior characterization, additive manufacturing, mechanical system modelling and performance optimization of energy converter.